China Instrument and Control Society
Instrumentation
INSTRUMENTATION, Vol. 11, No. 2, June 2024 https://doi.org/10.15878/j.instr.202400030

Article

Precision Machining Equipment Fault Diagnosis Based on CWT and Improved ResNeXt

Lichen Shi[1], Jiahang Guo[2], Haitao Wang[2,*]

[1] School of Mechanical and Electrical Engineering, Xi 'an University of Architecture and Technology, Xi' an, 710005

[2] Finishing Processing Laboratory, Xi 'an University of Architecture and Technology, Xi' an, 710005

[*] Corresponding author email: 17513161703@163.com

Abstract: A fault diagnosis method based on continuous wavelet transform and improved multi-dimensional residual network was proposed to solve the problem that the working environment of precision machining equipment is very complicated, and the fault characteristic signal is weak and hard to extract. Firstly, the best wavelet base Cmor 3-3 is selected by comparing 6 different wavelet base types. Secondly, continuous wavelet transform (CWT) is applied to the acquired original vibration signal to generate the feature map and process the gray level. Finally, the improved ResNeXt network is used to diagnose faults in precision machining equipment. The experimental results show that the proposed CWT and the improved ResNeXt algorithm have high accuracy in identifying precision machining equipment faults in complex environments, with an average accuracy of 99.4%.

Keywords: complex working environment; ResNeXt; precision working equipment

Citation: Shi, Lichen, Jiahang Guo, and Haitao Wang. "Precision Machining Equipment Fault Diagnosis Based on CWT and Improved ResNeXt." Instrumentation 11, no. 2 (2024). https://doi.org/10.15878/j.instr.202400030.

0 Introduction

Precision machining is an essential part of machining production, but its complex working environment makes its state difficult to identify and fault characteristics difficult to extract. For example, in the machining process, the vibration of the tool system and the coupling among various environmental factors make the final signal very complex. Extracting the effective state signal, namely the fault signal, from the background of complex environmental coupling is an important study for the state monitoring of finishing equipment[1]. Many scholars have researched the condition monitoring of processing equipment under a complex background. Yu Chunyu[2] et al. proposed an intelligent fault diagnosis method for bearings in complex environments based on EMD-AR and an improved broad learning system(BLS). Zhang Ruicheng[3] et al. proposed a fault diagnosis method for wind power converters under the complex background of Local Mean Decomposition (LMD) energy entropy and positioning analysis switch. However, both the empirical mode decomposition (EMD) and LMD will have endpoint effects and mode aliasing phenomena. Li[4] proposed a based on experience wavelet transform (EWT) -synchronous extraction complex environment equipment bearing fault identification technology, which can effectively diagnose the degree of fault and damage, EWT overcome the EMD method of under envelope and envelope and mode mix problem, but EWT need to define the filter set boundary, poor adaptability, and consume much time.

In recent years, due to the excellent ability of deep learning algorithms, which can mine the advantages of potential features of data well, more and more scholars have used deep neural networks to conduct fault diagnosis of devices in complex backgrounds. Li Weihua and et al. [5] used a deep confidence network (DBN) to directly learn the fault characteristics of mechanical equipment bearings from the original signal for fault diagnosis, realizing the fault classification of bearings and controlling the cost of DBN. Cao et al.[6] uses the long-term and short-term memory network (LSTM) for fault diagnosis and identification of mechanical equipment in complex environments. Chen[7] et al. discrete the fault signals of mechanical equipment in complex working environments

to obtain the two-dimensional time-frequency information then input it to the convolutional neural network (CNN) for classification and identification. All the above methods have achieved good results. However, static convolution is used in the network structure of these deep neural networks, and parameters cannot be adjusted adaptively according to different situations. Corresponding weights can be assigned to the convolution kernel to extract features fully.

Based on the above factors, this paper proposes a fault diagnosis method for precision machining equipment based on CWT and improved ResNeXt. Compared with EMD and LMD, CWT has the ability to represent the local characteristics of signals in both the time domain and frequency domain. CWT can decompose the signals into different frequencies and scales, which can more effectively handle the vibration signals in complex backgrounds. The improved multi-dimensional residual network into the fault diagnosis of precision machining equipment in complex background can effectively avoid the gradient descent problem caused by the stacking of model layers and then realize the fault diagnosis of precision machining equipment in complex environment.

1 Establishment of a fault diagnosis model for precision equipment

1.1 The wavelet transform

Wavelet transform is very suitable for analyzing non-stationary nonlinear fault signals in complex backgrounds, and vibration signals of precision machining equipment are often nonlinear in complex environments, and wavelet transform can decompose vibration signals from two scales of time and frequency. So this paper uses wavelet transform and its time and frequency map to carry out the fault diagnosis of precision machining equipment in a complex environment. Continuous wavelet transform (Continuous wavelet transform, CWT) transforms the original vibration signal data into a two-dimensional time-frequency diagram. The essence of continuous wavelet transforms lies in the translation and scale transformation of the wavelet base to approximate the original data as much as possible. For $\forall a \neq 0$, $b \in R$, then the wavelet basis function of the dependent parameters a, and b can be expressed as:

$$\Psi(a,b)(t) = \frac{1}{\sqrt{|a|}} \psi\left(\frac{t-b}{a}\right) \tag{1}$$

where a is the scale factor that affects the scaling of the function $\Psi(t)$; b is the displacement factor that affects the translation of the function $\Psi(t)$.

It meets the allowable conditions:

$$C_\psi = \int_{-\infty}^{+\infty} \frac{|\Psi(\omega)|^2}{|\omega|^2} d\omega <= +\infty \tag{2}$$

If the signal $f(t) \in L^2(R)$ represents the whole body of the energy-limited signal, the wavelet transformation of $f(t)$ is:

$$W_f(a,b) = \int_{-\infty}^{+\infty} f(t)\overline{\Psi(a,b)}(t)dt \tag{3}$$

where $\overline{\Psi(a,b)}(t)$ is the conjugate complex of the wavelet basis function $\Psi(a,b)(t)$.

1.2 Improve the multi-dimensional residual network

1.2.1 Dynamic convolution

Dynamic convolution is a method proposed by Chen et al. to aggregate multiple parallel convolution kernels of the dynamics according to the attention mechanism. Compared with the traditional static convolution layer, dynamic convolution does not use a single convolution kernel on each layer but adaptively adjusts the size of the convolution kernel according to samples of different sizes.

The parameters of the traditional perceptron do not change when the model runs, and the results are as follows:

$$y = g(W^T x + b) \tag{4}$$

where x and y represent the input and output respectively, g is the activation function, W^T is the transpose of the weight matrix, and b is the bias vector.

The dynamic perceptron updates the assigned parameters by integrating multiple linear functions $\widetilde{W}_k^T x + \tilde{b}_k$ as follows:

$$y = g(W^T(x)x + \tilde{b}_k(x)) \tag{5}$$

$$\begin{cases} \widetilde{W}(x) = \sum_{k=1}^{K} \pi_k(x)\widetilde{W}_k \\ \tilde{b}_k(x) = \sum_{k=1}^{K} \pi_k(x)\tilde{b}_k \\ 0 \le \pi_k(x) \le 1, \sum_{k=1}^{K} \pi_k(x) = 1 \end{cases} \tag{6}$$

where K is the number of integrated linear functions, $\pi_k(x)$ is the attention weight of the k th integrated function generated, $\widetilde{W}_k$ and $\tilde{b}_k$ are the weight matrix and bias vector of the k th integrated function, respectively, and $W^T(x)$ and $\tilde{b}_k(x)$ represent the weighted weight matrix and weighted bias vector, respectively.

1.2.2 Multi-dimensional residual network

ResNeXt[8] is an improved network based on ResNet[9], which adds a branching structure to the ResNet network model and divides the number of convolution kernels of the ResNet network into several groups, thus increasing the width of the residual network, but does not increase the parameters and computation of the network. ResNeXt The basic module is shown in Fig.1.

ResNeXt Network split-conversion-merge form can be expressed as:

$$R(x) = \sum_{i=1}^{c} T_i(x) \tag{7}$$

where T_i is the same topology, c is the number of identical branches in a module, c is usually called the

cardinality, and the value of c can be any integer.

ResNeXt The network can learn the spatial characteristics of signals deeper and improve the model performance with a multi-scale structure. After extracting the signal features from the ResNeXt model, the vector is flattened to one dimension by the global average pooling. Finally, using the Softmax function of the fully connected layer, the output is transformed as below to complete the fault diagnosis of the precision machining equipment.

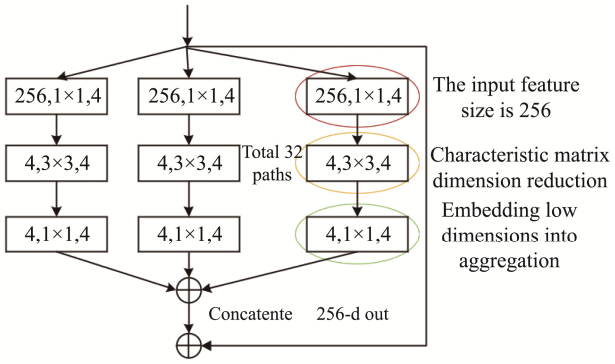

Fig.1 ResNeXt network module

$$P(i) = softmax(x_i) = \frac{exp(x_i)}{\sum_{j=1}^{c} exp(x_j)} \tag{8}$$

where: $P(i)$ is the probability value of the i th sample, and $0< P(i) <1$.

In order to improve the generalization performance and feature extraction ability of ResNeXt network model, this paper increases the number of ResNeXt network layers to 50 layers, as shown in Fig.2, the number of branches is increased to 32 groups, and the number of convolution cores in each group is 4 (32×4d).

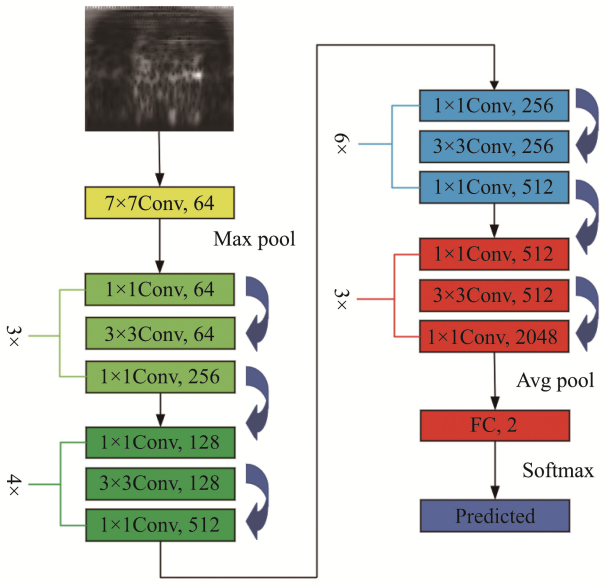

Fig.2 ResNeXt-50 network structure diagram

Compared with the conventional ResNet network, the depth and width of the model are enhanced, but due to the branching structure, the number of parameters of the model does not increase, and the number of ResNeXt network layers is increased to 50 layers, and the feature extraction ability of the model is further enhanced.

1.2.3 Improvement of multi-dimensional residual networks

In order to make full use of the powerful feature extraction ability of the dynamic convolutional kernel and extract more effective fault features, the dynamic convolution kernel is introduced into the multi-dimensional residual network, so that the original ResNeXt network has the profound feature extraction ability. The residual block structure embedded in the dynamic convolutional kernel is shown in Fig.3. In order to give full play to the effect of the dynamic convolution kernel, the dynamic convolution kernel is added to the output and branch structure of each layer of the network, so as to increase the feature extraction ability of the ResNeXt network.

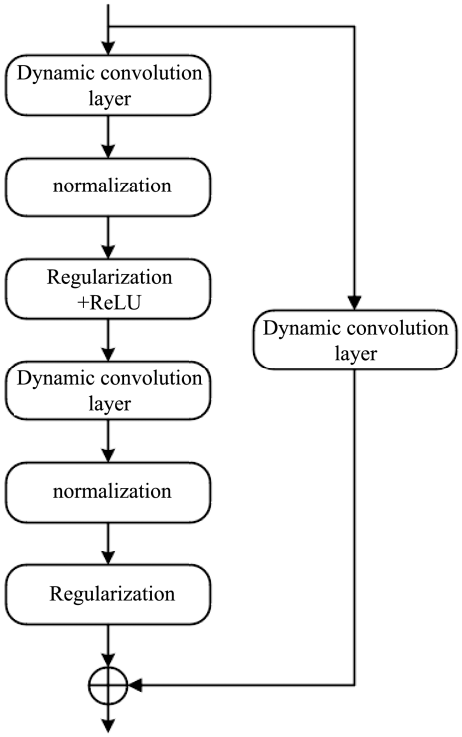

Fig.3 For the improved ResNeXt residual blocks structure

2 Experimental design

2.1 Composition of the experimental platform

In order to verify the proposed model in the complex environment of precision machining equipment fault diagnosis reliability, the experiment selection on high precision processing equipment inadvertently lathe[10], the working principle is the motor with the hollow shaft rotation, and then drive the front cutter high-speed rotation, to complete the wire cutting processing, structure as shown in Fig.4 (a). Install two acceleration sensors to the front and

rear bearings and arrange the sensors as shown in Fig.4 (b). The signal acquisition instrument collected the vibration signal, the cutting speed was selected as 480 r/min, the cutting depth was selected as 0.6 mm, and the sampling frequency was set as 8192 Hz.

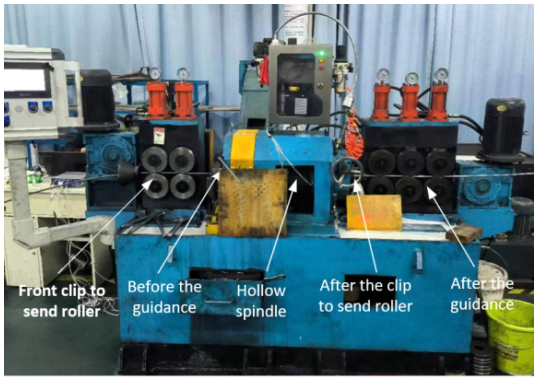

(a)Unintentional lathe structure

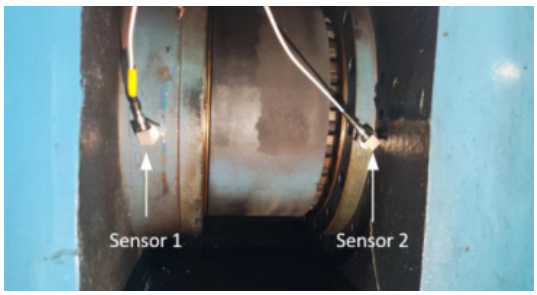

(b)Sensor point position

Fig.4 Experimental platform

2.2 Different fault implantation methods

In the daily processing production, the most common fault is the front clip too tight and the knife tip is not consistent. The front clamping will cause the workpiece to be tightly squeezed tightly by the front clamping roller. When the workpiece is pressed, the running state of the workpiece in the feeding process is volatile, which leads to abnormal vibration. As shown in Fig.5, the front clip pressure gauge shows the tightness of the front clip. For the overtight fault before implantation, increase the pressure of the front clamp roller by adjusting the front clamp pressure control button on the control panel.

Fig.5 Fault implantation experiment with the inconsistent protruding length of the knife tip

The method of implantation is to add a metal sheet of 0.17mm thickness to the no. 4 tool, as shown in Fig.6. When the length of the knife tip is not consistent, the cutting force of the four knives will not be consistent, and the cutting is easy to produce large vibration, thus affecting the cutting quality.

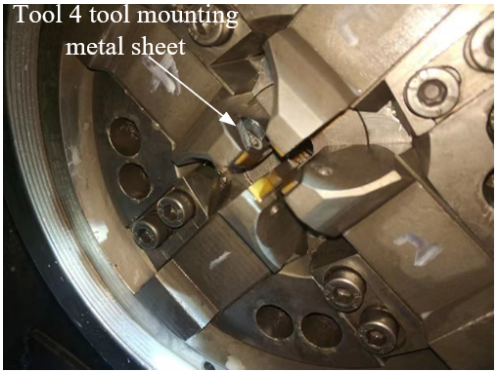

Fig.6 Fault implantation experiment with the inconsistent protruding length of the knife tip

2.3 Data preprocessing

Data preprocessing mainly contains two parts: generating feature maps and image fusion. For one-dimensional acceleration vibration signal data, this paper uses the overlap sampling method to expand the data set sample, that is, there is an overlap between the n th segment sample and the n+1 segment sample. The relationship between the length, step length and the total number of samples is shown in Equation 9.

$$n = \frac{N - Sample}{stride} + 1 \tag{9}$$

where N represents the length of the acceleration vibration signal for a certain fault state, n represents the total number of the samples available, stride represents the length of the overlapping sampling, and Sample represents the length of each segment. On the length selection of each segment, the selected sample length is 1024, the number of overlapping sampling is 512, the acceleration vibration signal length of each fault state is 122880, the number of each fault sample generated by overlapping sampling method is 500, and the size of feature image is 128×128. The characteristic diagram of each fault state is shown in Fig.7.

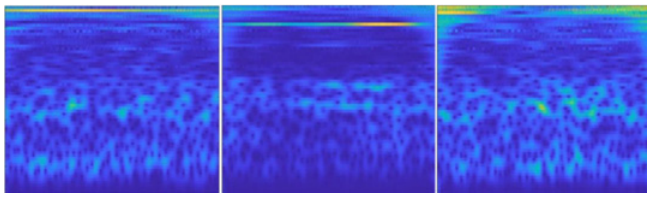

The tip of the knife is inconsistent | The front clip is too tight | Normal

Fig.7 Characteristic pattern

It can be seen from the figure that the two-dimensional time-frequency feature map generated

by the unintentional lathe fault experimental data cannot see the large difference. Therefore, it is necessary to use the deep learning method to identify further and extract the feature of the unintentional lathe fault feature map.

2.4 Fault process based on CWT and improved ResNeXt

The fault diagnosis process of precision machining equipment based on CWT and improved ResNeXt is shown in Fig.8. The specific steps are described as follows.

(1) Signal preprocessing: convert the unintentional lathe acceleration vibration signal data set sample into CWT feature map, and divide the test set sample and the training set sample to prepare for the subsequent model training and testing.

(2) Model design and training: set up relevant network parameters such as learning rate, optimizer and loss function according to the pre-build of the improved ResNeXt network model. The training set sample input to the model forward propagation path in the loss error, determine the error meet the requirements, if not meet the error backpropagation, adjust the network parameters, If the model training parameters are satisfied, the model is trained and tested.

(3) Fault classification identification: after the improved multi-dimensional residual network model proposed in this paper is trained, the test set is input into the trained network to identify the faults of the test samples, and the fault classification accuracy is finally obtained.

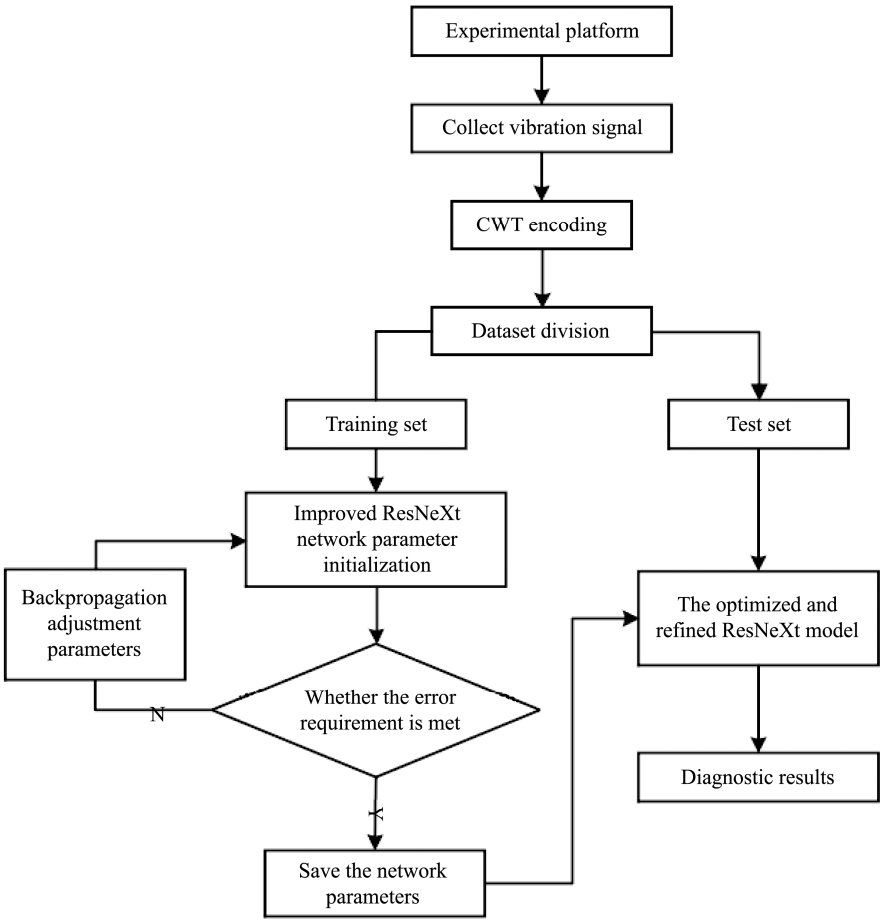

Fig.8 Fault diagnosis process based on CWT and improved ResNeXt

3 Analysis of the experimental results

3.1 Effect of small wave groups

The wavelet basis function is crucial to the image generation quality of the feature map[11], choosing the appropriate wavelet basis function can increase the signal-to-noise ratio of the feature map and make the image clarity higher. The complex wavelet basis function can consider both the amplitude frequency characteristics and phase frequency characteristics, so the complex wavelet base ComplexMorlet is chosen as the parent wavelet. The basic form of this wavelet is cmorfb-fc (where fb is the bandwidth width and fc is the center frequency). In order to obtain the best feature map, 6 types of ComplexMorlet wavelet are taken as candidates, as shown in Table 1.

In order to compare the quality of feature graphs generated by different wavelet basis functions, sample feature graphs generated by 6 wavelet bases were input into the improved multidimensional residual network and trained for 20 times. The accuracy obtained was

shown in Fig.9.

Table 1 9 wavelet base candidates

Number	Wavelet base type	Wavelet basis
1	Cmor	Cmor1-1
2	Cmor	Cmor2-2
3	Cmor	Cmor3-3
4	Cmor	Cmor4-4
5	Cmor	Cmor5-5
6	Cmor	Cmor6-6

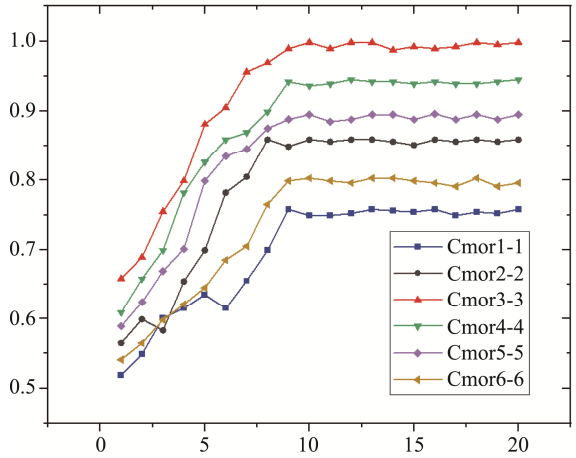

Fig.9 Line plot of the results of different wavelet base experiments

It can be seen from the figure that the fault classification accuracy of the Cmor 3-3 wavelet basis function is the highest, so the Cmor 3-3 wavelet basis function is chosen as the wavelet base of the continuous wavelet transform.

3.2 Impact of different pre-trained models

In order to verify the performance of the proposed model in this paper, the three deep learning models in the deep learning field are based on the same data set. To reduce the influence of chance factors, when dividing the training set and the test set, 10 random partitions were performed, using each set of data for independent training and testing, to record the experimental results separately. The results of 10 experiments were used as performance evaluation indicators for comparative validation, and the specific results are shown in Fig.10, and the mean accuracy and standard deviation are shown in Table 2. Among them, the accuracy of the GoogLeNet[12] model is poor, only reaching 91.92%, because the model simply stacks multiple convolution layers, and it is difficult to extract complex data features effectively. ResNet The residual structure is added based on GoogLeNet to realize the cross-layer connection of each convolutional layer, and its accuracy is 3.53% higher than that of GoogLeNet. DenseNet[13] The dense residual connection module is added to realize the dense connection of each convolutional layer, and the accuracy is 1.5% higher than ResNet. However, the overall accuracy is low because the above models use a single network structure for feature extraction.

The method proposed in this paper can fully integrate the time-frequency features of the signal and extract the fault signals submerged by various noises in the complex background. The dynamic convolution kernel improves the feature extraction capability of the network, and the average test accuracy is 99.40%.The above results show that the deep learning model proposed here has obvious advantages over several other deep learning models.

Table 2 Average accuracy and standard deviation

Accuracy rate /%	The method of this paper	GoogLeNet	ResNet	DenseNet
Train	99.70±0.15	92.92±0.23	96.58±0.82	97.35±0.09
Test	99.40±0.13	91.92±0.89	95.45±0.53	96.95±0.26

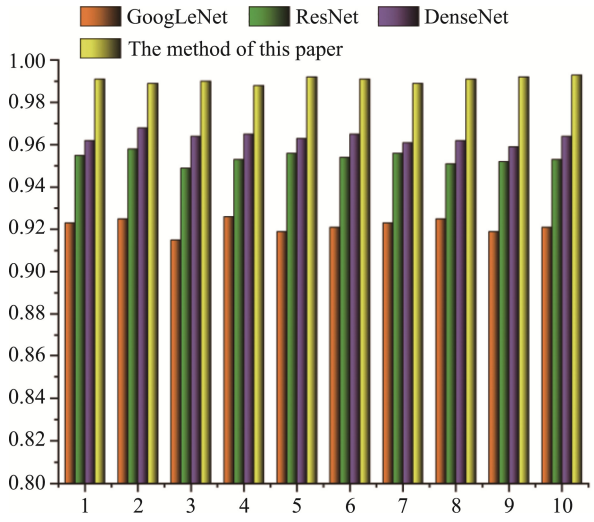

Fig.10 Test accuracy for the ten experiments

3.3 Comparison of different image encoding methods

In order to verify the advantages of using the CWT image coding feature map, the following graph coding method is compared with the method in this paper. ①: Use continuous wavelet transform to convert a one-dimensional vibration signal into a time-frequency map, and input it to the improved ResNeXt network. ②: Convert the one-dimensional acceleration vibration signal into a Markov transition field, Markov Change Field (MTF) image. ③: THE method of literature[14] is used to convert the acceleration vibration signal into the Graham Angular Field-gram angle field (GAF) image, and the GAF feature image is used as the input to the improved ResNeXt network. All the above methods adopt overlapping sampling method, and the data are divided into training set and test set in a ratio of 4:1, and the image size is set to 128×128. Three types of image coding are selected, and one fault type is displayed, as shown in Fig.11.

CWT MTF GAF

Fig.11 Three kinds of image encoding methods

Taking the above three images as inputs to the network model, it can be seen from Fig.12 that the fused CWT feature map has the highest accuracy, with the average accuracy of 99.4% after 20 training, while the average accuracy of MTF and GAF can only reach 92.5% and 86.4% after 20 training, respectively. Therefore, the above experimental results show that the fault diagnosis model of deep learning precision machining equipment has high accuracy and stability.

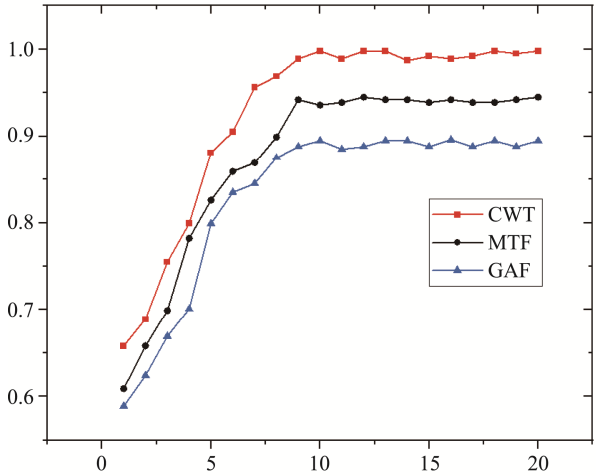

Fig.12 Experimental results for other image encoding methods

3.4 Fault diagnosis experiment of migration across working conditions

In actual work, the working conditions of the unintentional lathe often change, so it is necessary to verify the classification accuracy of the proposed fault diagnosis model under different working conditions. According to different working conditions, the experimental data set of centerless lathe is divided into three groups, in which working condition A is centerless lathe speed 480 r/min, feed speed 0.5 m/min. Under working condition B, the speed is 530 r/min. Working condition C is speed 580 r/min. In each group of data, there were 500 sample data of each component state, a total of 1500, and the training set and test set were divided according to the ratio of 8 : 2. See Table 3.

Using source domain data, the constructed model, the ResNet model and the ResNeXt model and Dy-ResNeXt model .The migration experimental results of each model under different working conditions are shown in Fig.13.A-B of the data in the figure represents the source domain data of the data set with working condition A as the data set, and the target domain data of the data set with working condition B as the data set. A-C indicates that condition A is the source domain of the data set, condition C is the target domain of the data set, and so on.

Table 3 No intentional lathe working condition fault

Fault type	normal	The tip of the knife is inconsistent	The front clip is too tight
Fault label	1	2	3
Condition A	500	500	500
Condition B	500	500	500
Condition C	500	500	500

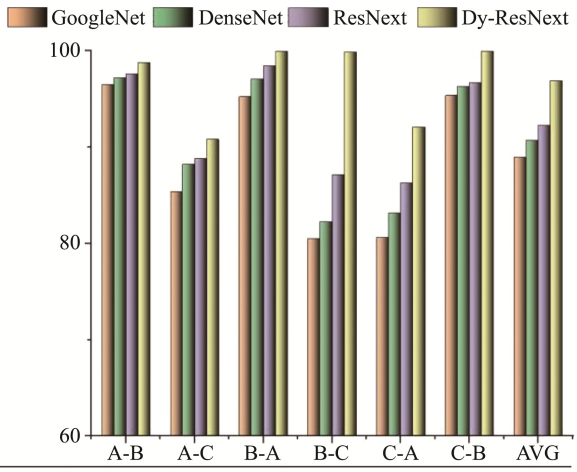

	A-B	A-C	B-A	B-C	C-A	C-B	AVG
GoogLeNet	96.51	85.42	95.26	80.53	80.67	95.38	88.96
ResNet	97.23	88.23	97.12	83.29	83.18	96.35	90.73
ResNeXt	97.59	88.86	98.46	87.11	86.31	96.73	92.29
Dy-ResNeXt	98.79	90.84	99.98	99.92	92.12	99.98	96.94

Fig.13 Experimental results across working conditions

In order to illustrate the classification effect of the model under cross-working conditions, 80 samples were taken as the test set. The experimental results are shown in Fig.13. Judging from the classification results in the above figure, the proposed methods in this paper have higher accuracy than the models obtained by the other three methods. Taking source domain data as working condition B and target domain data as working condition A as an example, the fault identification accuracy of Dy-ResNeXt is 99.92%, which is 1.13% higher than that of working condition A to working condition B and 9.08% higher than that of working condition A to working condition C. The accuracy of this model is 1.56% higher than that of ResNet model and 1.2% higher than that of ResNeXt model. The above models all use a single network structure to extract fault features, so the fault diagnosis accuracy of precision machining equipment in complex environments is slightly low. The proposed method can fully extract the feature information of fault signals in complex backgrounds, and the dynamic convolution kernel is integrated into the ResNeXt network to improve the expression ability of the model significantly. Therefore, the reliability of the model in

fault diagnosis of precision machining equipment under complex environment is verified.

4 Summary

In view of the working environment of precision machining equipment in processing and production is very complex and the problem is difficult to identify, this paper, a fault diagnosis algorithm (CWT-Dy-ResNeXt) of precision machining equipment based on continuous wavelet transform and improved multi-dimensional depth residual network is combined, and then the effectiveness of this method is proved through experimental research. The model presented in this paper has the following advantages over the other network models.

(1) With CWT, CWT and the images have time and frequency domain features compared with MTF and GAF. In addition, the complex wavelet basis function ComplexMorlet is used as the parent wavelet, which can analyze the characteristics of the signal from the amplitude-frequency characteristics and phase frequency characteristics of the vibration signal, and select the best wavelet base through the comparison of different wavelet basis functions.

(2) ResNeXt has stronger than ResNet generalization performance and feature extraction ability, ResNeXt network adopts multiple branch structure, under the condition of guarantee model parameters do not increase, improve training accuracy, dynamic convolution kernel can adapt according to the sample size adaptive convolution kernel, increased the size of the model in the complex environment of precision machining equipment the reliability and stability of fault diagnosis.

Author Contributions:

Shi Lichen: Conceptualization, data management, capital acquisition. Guo Jiahang: Formal analysis, investigation, data visualization, and paper writing and review. Wang Haitao: Provide resources, software, supervision, verification.

Funding Information:

This research obtained fund project: Funding from the Key Research and development plan of Shaanxi Province "Research on key problems of surface finishing for Aerospace Fastener" (2023-YBGY-386).

Data Availability:

This data is from the centerless lathe fault data set collected by the finishing processing laboratory of Xi 'an University of Architecture and Technology, and is not a public data set.

Conflict of Interest:

The authors declare no competing interests.

Dates:

Received 17 July 2023; Accepted 17 December 2023; Published online 30 June 2024

References

[1] Quan Quan, Cui Gen, Zhao Zhiyao, etc. Several thoughts on health assessment in complex systems [J]. Journal of Jilin University (Engineering Edition), 2023, 53 (03): 601-28.

[2] Yu Chunyu, Zhang Wentao, Zhang Qinghai, etc. Based on EMD-AR and improved Width Learning System [J]. Chinese Journal of Electrical Engineering, 1-13.

[3] Zhang Ruicheng, Bai Xiaolei, Dong Yan, et al. Open circuit fault diagnosis of wind power converter based on LMD energy entropy and location analysis [J]. Journal of Solar Energy, 2023, 44 (06): 484-94.

[4] Li Zhinong, Liu Yuefan, Hu Zhifeng, et al. Empirical wavelet transform-synchronous extraction and its application in rolling bearing fault diagnosis [J]. Journal of Vibration Engineering, 2021, 34 (06): 1284-92.

[5] Li Weihua, Shan Waiping, Zeng Xueqiong. Bearing fault classification and identification based on the deep belief network [J]. Journal of Vibration Engineering, 2016, 29 (02): 340-7.

[6] CAO L, ZHANG J, WANG J, et al. Intelligent fault diagnosis of wind turbine gearbox based on Long short-term memory networks; proceedings of the 2019 IEEE 28th International Symposium on Industrial Electronics (ISIE), F, 2019 [C]. IEEE.

[7] CHEN R, HUANG X, YANG L, et al. Intelligent fault diagnosis method of planetary gearboxes based on convolution neural network and discrete wavelet transform [J]. Computers in industry, 2019, 106(48-59.

[8] XIE S, GIRSHICK R, DOLLáR P, et al. Aggregated residual transformations for deep neural networks; proceedings of the Proceedings of the IEEE conference on computer vision and pattern recognition, F, 2017 [C].

[9] HE K, ZHANG X, REN S, et al. Deep residual learning for image recognition; proceedings of the Proceedings of the IEEE conference on computer vision and pattern recognition, F, 2016 [C].

[10] Shi Lichen, Shao Xianzhong, Wang Haitao, et al. Surface roughness prediction based on sensitive factor selection and residual network [J]. Computer Integrated Manufacturing system, 1-19.

[11] Chen Renxiang, Zhou Jun, Hu Xiaolin, et al. Rotational mechanical fault diagnosis method based on deep Q learning and continuous wavelet transform [J]. Journal of Vibration Engineering, 2021, 34 (05): 1092-100.

[12] SZEGEDY C, LIU W, JIA Y, et al. Going deeper with convolutions; proceedings of the Proceedings of the IEEE conference on computer vision and pattern recognition, F, 2015 [C].

[13] HUANG G, LIU Z, VAN DER MAATEN L, et al. Densely connected convolutional networks; proceedings of the Proceedings of the IEEE conference on computer vision and pattern recognition, F, 2017 [C].

[14] Wang Haitao, Guo Yifan, Shi Lichen. Fault method of rolling bearing based on SC-ResNeSt and frequency angle field [J]. Computer Integrated Manufacturing System, 1-21.